

## SYNTHESIS AND CHARACTERIZATION OF POLYMER/IRON OXIDE NANOCOMPOSITE FOR OPTICAL ANALYSIS

Okafor L. U<sup>1</sup> and Ottih I.E<sup>2</sup>

<sup>1</sup>Department of Physics and Industrial,  
Nnamdi Azikiwe University, Awka, Anambra state, Nigeria.

<sup>2</sup>Department of Industria Physics,  
Chukwuemeka Odumegwu Ojukwu University, Uli,  
Anambra State, Nigeria

### ABSTRACT

*In this paper PANI and Fe<sub>2</sub>O<sub>3</sub> nanoparticles were successfully synthesized by chemically oxidative polymerization of aniline in the presence of hydrochloric acid using ammonium persulphate as an oxidizing agent. The optical properties were characterized using spectrophotometer. Optical properties investigated are absorbance, transmittance, reflectance, refractive index, extinction coefficient and energy band gap. The samples revealed high transmittance and low absorbance across the whole regions. At VIS and NIR regions, the nanocomposite revealed high refractive index and high extinction coefficient at UV and VIS regions. Energy band gap of PANI and Fe<sub>2</sub>O<sub>3</sub> are 2.69ev and 2.15ev while the energy band gap of the PANI/Fe<sub>2</sub>O<sub>3</sub> nanocomposite decreases as the concentration of the iron oxide increases in the nanocomposite fabricated.*

**Keywords** – Conducting polyaniline, Polyaniline/Fe<sub>2</sub>O<sub>3</sub> nanocomposite, Optical properties

### 1. INTRODUCTION

Nanoparticles are particles which are 1 to 100 nanometers in size. Metal oxides nanoparticles have been investigated by some researchers in the past years. Investigations on nanoparticles are on the high side because of their special physical and chemical properties different from the bulk materials (Reddy et al, 2007). Their special properties are high surface area, quantum size effects and lower sintering temperature. Presently, polymer/metal oxide nanocomposites are important class of materials in the area of nanotechnology. Polyaniline (PANI) is the most attractive conducting polymer among the other conducting polymer because of its environmental stability, easy synthesis and low cost (Majid et al, 2007). The composites of conducting polymers and inorganic materials are of great interest because they exhibit a good range of electrical, optical and magnetic properties (Tang et al, 1999). Therefore, the optical properties of the nanocomposites of PANI/Fe<sub>2</sub>O<sub>3</sub> are investigated in this paper.

### 2. EXPERIMENTAL

#### 2.1. Materials

Materials used for the fabrication of polyaniline /iron oxides nanocomposite including reagents and laboratory apparatus are; (i) Iron (III) chloride hexahydrate (FeCl<sub>3</sub> · 6H<sub>2</sub>O), (ii) Iron (II) tetraoxosulphate (VI) heptahydrate (FeSO<sub>4</sub> · 7H<sub>2</sub>O), (iii) Aniline (C<sub>6</sub>H<sub>5</sub>NH<sub>2</sub>), (iv) Hydrochloric acid (HCl), (v) Ammonium persulphate ((NH<sub>4</sub>)<sub>2</sub>S<sub>2</sub>O<sub>8</sub>), (vi) Ammonium hydroxide Solution (NH<sub>4</sub>OH), (vii) Absolute Ethanol (C<sub>2</sub>H<sub>6</sub>O), (viii) Whatman filter paper

(110 mm), (ix) Magnetic stirrer with heater, (x) Digital weighing balance and (xi) 250 ml beakers.

### 2.1 Preparation of Iron Oxide nanoparticles

Co – precipitation of iron oxide nanoparticles was obtained by mixture of iron (III) chloride and iron (II) tetraoxosulphate (VI) in the 2:1 molar ratio. The 100ml of ferric chloride and 50ml of ferrous sulfate solutions were transferred to a 250ml beaker, the mixture was then heated up to 60°C for 10 minutes. After heating, the solution was precipitated by drop – wise addition of ammonia solution with the rate of 1 mL per minute for 1 hour. The final solution was allowed to stay under continuous stirring on the magnetic stirrer at 60°C for another 1 hour. At end of the 2 hours, the beaker containing the solution was allowed to cool. Brown colored particles of iron oxides were precipitated. The brown colour suggests that iron (III) oxide ( $Fe_2O_3$ ) was formed. These particles were then separated from the solution by using a strong magnet and then were washed many times with distilled water. The powder was then dried in hot air oven at 100°C for 24 hours. The standard sample obtained was labelled  $A_1$ . The overall reaction can be written as



### 2.3. Preparation of polyaniline nanoparticles

3. The polymerization of aniline to form the desired polyaniline was based on mixing aqueous solutions of aniline hydrochloride (100ml of aniline solution was dissolved in 500ml of 0.1M of HCl) and ammonium persulfate – hydrochloride (18.25 g of ammonium persulfate mixed with 100 ml of 1.0M of HCl) at room temperature. Firstly, 100 ml of aniline hydrochloride solution was stirred for 30 minutes in an ice bath followed by a drop – wise addition of 20ml of ammonium persulfate – hydrochloride at drop rate of 1 drop per minute. The solution was subjected to further magnetic stirring in the ice bath for another 30 minutes. The final solution was removed from the ice bath and allowed to age for 24 hours to polymerize completely. The separation of PANI hydrochloride precipitate was done by filtration using whatman filter paper. The precipitate was washed several times with 1.0ml HCl, similarly with acetone and finally with distilled water. Polyaniline hydrochloride powder was dried in air and then in vacuum at 60°C for 24 hours. Polyaniline prepared under these reaction and processing conditions are further referred to as “standard” samples.

### 2.4. Preparation of Polyaniline – Iron oxide (PANI/ $Fe_2O_3$ ) nanocomposites

Synthesis of the Polyaniline– iron oxide nanocomposites were carried out by in-situ polymerization method. 100ml of aniline – hydrochloride was stirred with a magnetic stirrer for 30 minutes in an ice bath. 0.5 g of iron oxide nanoparticles fabricated were dispersed in the above solution with vigorous stirring for 30 minutes in order to keep the iron oxide homogeneously suspended in the solution. To this solution, 20ml of ammonium persulfate hydrochloride was added drop – wise with drop rate of 1 drop per minute. The final solution was removed from the ice bath and allowed to age for 24 hours to completely polymerize. The precipitate was filtered then washed with 1.0m hydrochloric acid, acetone, water for many times and finally dried in a hot air oven at 60°C for 24 hours. In this way, Polyaniline – iron

oxide nanocomposites containing various masses of 1.0g, 1.5 g, and 2.0 g  $\text{Fe}_2\text{O}_3$  in PANI were synthesized using the same procedures.

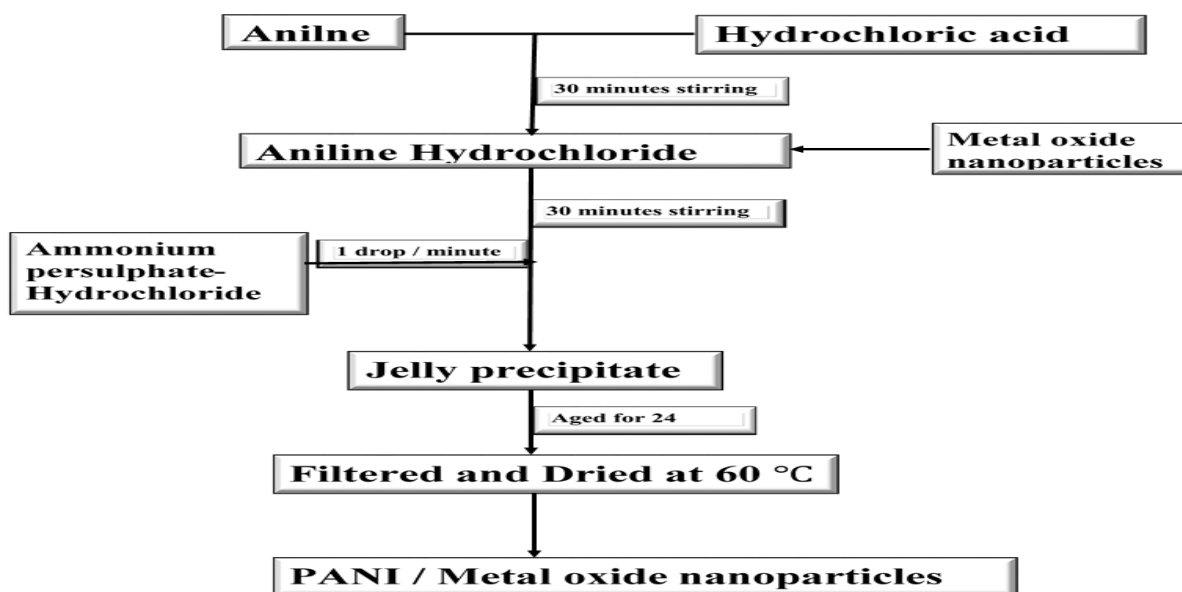


**Figure 1: Flowchart of the method of synthesis of Polyaniline – Metal oxide nanoparticles**

#### 4. RESULTS AND DISCUSSION

The optical results obtained from the investigation of the fabricated Polyaniline, iron oxide and their nanocomposite are presented and discussed respectively. The optical investigation was carried out on the nanoparticles and nanocomposites fabricated. Optical absorption spectra of Polyaniline, iron oxide and their nanocomposite were studied using spectrophotometer within ultraviolet (UV) region of (250 nm to 390 nm), visible light (VIS) region of (400 nm to 700 nm) and near infrared (NIR) region of (710 nm to 800 nm) with a scanning speed of 400 nm/min. Other optical properties such as transmittance, reflectance, refractive index, extinction coefficient and optical band gap were evaluated. According to Gul *et al.*, (2013), absorption spectroscopy is a valuable tool to detect the presence of polyaniline salts (conducting state) and its base (insulating state)

##### 3.1. Optical properties of polyaniline, iron oxide and polyaniline – iron oxide (PANI/ $\text{Fe}_2\text{O}_3$ )

###### 3.1.1. Absorbance

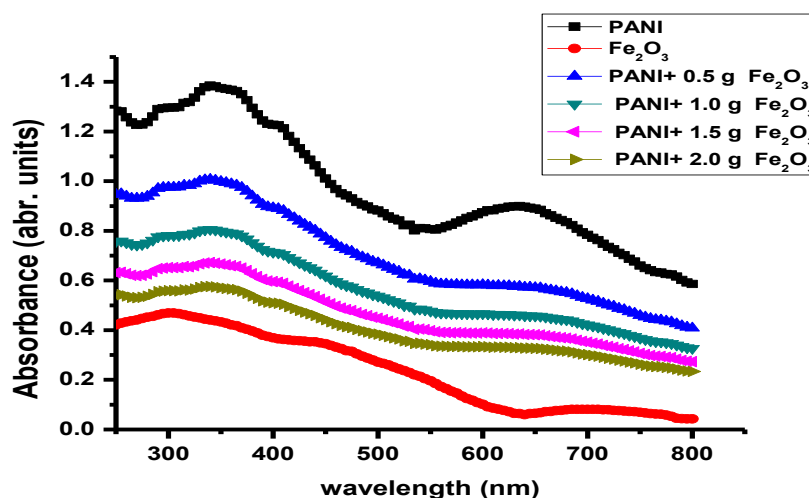


**Figure 2: Plot of Absorbance against wavelength for polyaniline (PANI), iron oxide  $\text{Fe}_2\text{O}_3$  and polyaniline – iron oxide nanocomposites**

Figure 2 shows the plot of absorbance against wavelength of electromagnetic radiation for polyaniline, iron oxide and polyaniline – iron oxide nanocomposites respectively. The absorbance of the films decreases with increase in wavelength within the UV region. The UV – VIS spectra of deposited films as show in Figure 2 has peak values at some wavelengths which depict some characteristics of a polyaniline film when subjected to electromagnetic radiations. Absorbance spectrum of pure PANI shown in Figure 2 reveals two prominent broad absorbance peaks. A broad peak between 335 nm and 345 nm represent aniline component and conductive ability of polyaniline (Vadiraj and Belagali, 2015). The peak is attributed to the transition of electrons from the highest occupied molecular orbital (HUMO) to the lowest unoccupied molecular orbital (LUMO) which is related to  $\pi - \pi^*$  electron transition of the benzenoid rings (Al – Daghman, 2019; Mota *et al.*, 2019, Hasoon and Abdul – Hadi, 2018; Karaoglan and Bindal, 2018; Gul *et al.*, 2013). Similar results were obtained by (Canales *et al.*, 2014; Abdulla and Abbo, 2012; Thanpicha *et al.*, 2008; Yang *et al.*, 2004). Another broad peak between 625 nm and 640 nm confirms the formation of polaron lattice which represents the protonation stages of polyaniline chains. The band is assigned to exit on in the quinoid ring which is responsible for charge transfer from adjacent benzenoid rings with each other contributing half electron on average (Han *et al.*, 2009; Yang *et al.*, 2007). According to Yin and Ruckenstein (2000) and Roy *et al.*, (2002), peaks within these ranges are assigned to the polaron and bipolaron band transition for polyaniline. Absorbance of iron oxide shown in Figure 2 (red) reveals that the value of absorbance decreases as wavelength increases. The absorbance values within UV region range from 0.42 at 250 nm to a peak value of 0.47 at 310 nm. It then decreases to 0.37 at 395 nm. In VIS region, the absorbance values range from 0.37 nm at 400 nm to 0.08 at 700 nm. The absorbance decreases further to 0.04 at 800 nm. This result shows that the fabricated iron oxide nanoparticles moderately absorb radiation in the UV region and tends to low absorptions within VIS and NIR regions. The absorption peak in the near UV region arises from electronic transition associated with  $\text{Fe}_2\text{O}_3$  (Farahmandjou and Soflace, 2015). The result is in line with that of (Hassan *et al.*, 2018). They obtained absorption peak of between 286 nm and 296 nm for  $\text{Fe}_2\text{O}_3$  nanoparticles fabricated by biosynthetic route.

Also, our result corresponds to results obtained by (Klaczanova *et al.*, 2013 and Balamurugan *et al.*, 2014). Absorbance graph of PANI / 0.5g of  $\text{Fe}_2\text{O}_3$  show that the absorbance values range from 0.95 at 250nm to a peak value of 1.01 at 340 nm. It decreases slightly to 0.90 at 395nm. In VIS region, the absorbance values range from 0.89 at 400 nm to 0.53 at 700nm. In NIR region, the values range from 0.52 at 705 nm to 0.41 at 800 nm. Absorbance graph of PANI/1.0 g of  $\text{Fe}_2\text{O}_3$  shows that the absorbance values range from 0.76 at 250 nm to a peak value of 0.81 at 340 nm. It decreases slightly to 0.72 at 395 nm. In VIS region, the absorbance values range from 0.71 at 400 nm to 0.42 at 700 nm. In NIR region, the values range from 0.42 at 705nm to 0.33 at 800nm. Absorbance graph of PANI / 1.5g of  $\text{Fe}_2\text{O}_3$  shows that the absorbance values range from 0.63 at 250nm to a peak value of 0.67 at 335nm. It decreases slightly to 0.60 at 395 nm. In VIS region, the absorbance values range from 0.60 at 400nm to 0.35 at 700nm. In NIR region, the values range from 0.35 at 705nm to 0.27 at 800 nm. Absorbance graph of PANI / 2.0g of  $\text{Fe}_2\text{O}_3$  show that the absorbance values range from 0.54 at 250nm to a peak value of 0.57 at 340nm. It decreases slightly to 0.51 at 395nm. In VIS region, the absorbance values range from 0.51 at 400nm to 0.30 at 700nm. In NIR region, the values range from 0.30 at 705nm to 0.23 at 800nm. These results show that the absorbance of polyaniline – iron oxide nanocomposites decreases as amount of iron oxide nanoparticles increases. This may be as a result of low absorbing nature of iron oxide nanoparticles which confirms the presence of iron oxide particles in the polyaniline matrix.

### 3.1.2. Transmittance

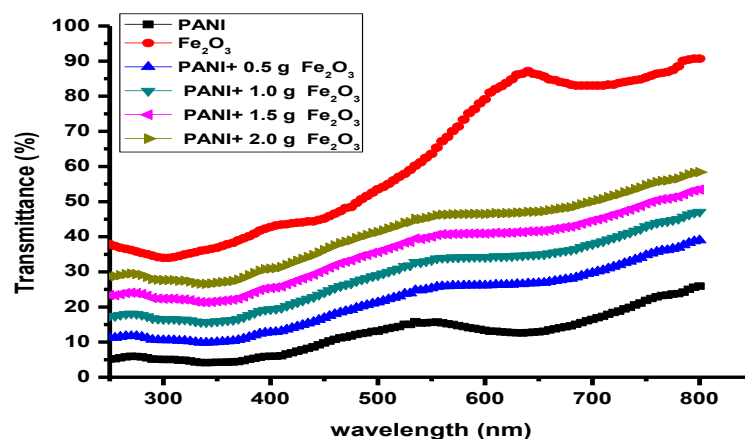


**Figure 3: Plot of Transmittance against wavelength for polyaniline (PANI), iron oxide  $\text{Fe}_2\text{O}_3$  and polyaniline – iron oxide nanocomposites**

Figure 3 shows the transmittance graphs plotted against wavelength for polyaniline particles, iron oxide nanoparticles and polyaniline – iron oxide nanocomposites with different iron oxide nanoparticle compositions. Transmittance values of polyaniline increase slightly from 5.21 % at 250 nm to 5.94 % at 270 nm and decreases to a value of 4.13 % at 340 nm. The value increases further from 5.88 % at 395 nm within the UV region. In VIS region, transmittance values of PANI range from 5.92 % at 400 nm to 16.90 % at 700 nm. In NIR region, the values range from 16.90 % at 705 nm to 25.94 % at 800 nm. Transmittance values of iron oxide nanoparticles range from 37.89 % at 250 nm to 33.97 % at 305 nm and increases further to 42.25 % at 395 nm within UV region. In VIS region, transmittance values range from

42.77 % at 400 nm to 83.04 % at 700 nm while in NIR region, the transmittance values increase further from 83.04 % at 705 nm to 90.66 % at 800 nm. Transmittance of PANI / 0.5 g of Fe<sub>2</sub>O<sub>3</sub> nanocomposites ranges from 11.30 % at 250 nm to 9.83 % at 340 nm which increases to 12.68 % at 395 nm in UV region. In VIS region, it ranges from 12.80 % at 400 nm to 29.73 % at 700 nm while in NIR region, the transmittance values are between 30.14 % at 705 nm and 39.01 % at 800 nm. Transmittance of PANI / 1.0 g of Fe<sub>2</sub>O<sub>3</sub> nanocomposites ranges from 17.48 % at 250 nm to 15.63 % at 340 nm which increases to 19.16 % at 395 nm in UV region. In VIS region, it ranges from 19.32 % at 400 nm to 37.89 % at 700 nm while in NIR region, the transmittance values are between 38.31 % at 705 nm and 47.09 % at 800 nm. Transmittance of PANI / 1.5 g of Fe<sub>2</sub>O<sub>3</sub> nanocomposites ranges from 23.31 % at 250 nm to 21.42 % at 345 nm which increases to 25.23 % at 395 nm in UV region. In VIS region, it ranges from 25.40 % at 400 nm to 44.54 % at 700 nm while in NIR region, the transmittance values are between 44.95 % at 705 nm and 53.39 % at 800 nm. Transmittance of PANI / 2.0 g of Fe<sub>2</sub>O<sub>3</sub> nanocomposites ranges from 28.78 % at 250 nm to 26.57 % at 340 nm which increases to 30.72 % at 395 nm in UV region. In VIS region, it ranges from 30.90 % at 400 nm to 50.00 % at 700 nm while in NIR region, the transmittance values are between 50.93 % at 705 nm and 58.40 % at 800 nm. These results show that the transmittance of polyaniline– iron oxide (PANI/Fe<sub>2</sub>O<sub>3</sub>) nanocomposites decreases as amount of iron oxide nanoparticles increases. This shows that incorporation of iron oxide into the polyaniline matrix improve the transmittive properties of polyaniline.

### 3.1.3 Reflectance

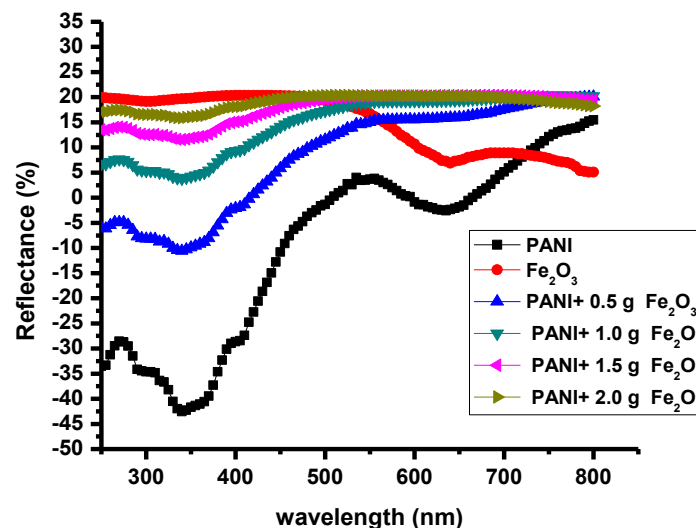


**Figure 4: Plot of Reflectance against wavelength for polyaniline (PANI), iron oxide Fe<sub>2</sub>O<sub>3</sub> and polyaniline – iron oxide nanocomposites**

Figure 4 shows the graph of reflectance plotted against wavelength for polyaniline nanoparticles, iron oxide nanoparticles and polyaniline – iron oxide nanocomposites respectively. The reflectance values of polyaniline nanoparticles range from –34.00 % at 250 nm to –29.00 % at 395 nm in UV region and from –29.00 % at 400 nm to –0.50 % at

505nm. Above 505 nm, reflectance becomes positive with value of 0.33 % at 510nm to a peak value of 3.84 % at 555nm. It further decreases to  $-0.60$  % at 660nm and then increases to 5.16 % at 700nm. In NIR region, reflectance values range from 5.90 % at 705nm to 15.50 % at 800 nm. Iron oxide has reflectance value of 20.00 % at 250nm which decreases slightly to 19.10 % at 305 nm before increasing to 20.30 % at 395 nm. In VIS region, reflectance values decrease from 20.30 % at 400nm to 8.89 % at 700nm. In NIR region, the decrease proceeds further from 8.89 % at 705nm to 5.08 % at 800nm. Reflectance of PANI / 0.5 g of  $\text{Fe}_2\text{O}_3$  nanocomposites ranges from  $-5.98$  % at 250 nm which decreases to  $-10.60$  % at 340 nm before increases to  $-2.38$  % at 395 nm in UV region. In VIS region, it ranges from  $-2.07$  % at 400 nm to 17.59 % at 700nm while in NIR region, the reflectance values are between 17.77 % at 705 nm and 20.11 % at 800nm. Reflectance of PANI / 1.0 g of  $\text{Fe}_2\text{O}_3$  nanocomposites ranges from 6.78 % at 250nm to 3.77 % at 340nm which increases to 9.08 % at 395 nm in UV region. In VIS region, it ranges from 9.28 % at 400nm to 19.96 % at 700 nm while in NIR region, the reflectance values increase slightly from 20.02 % at 705 nm to 20.20 % at 800 nm. Reflectance of PANI / 1.5 g of  $\text{Fe}_2\text{O}_3$  nanocomposites ranges from 13.50 % at 250 nm to 11.66 % at 345 nm which increases to 14.97 % at 395nm in UV region. In VIS region, it ranges from 15.09 % at 400nm to 20.34 % at 700nm while in NIR region, the reflectance values decrease slightly 20.32 % at 705 nm and 19.36 % at 800 nm. Reflectance of PANI / 2.0 g of  $\text{Fe}_2\text{O}_3$  nanocomposites ranges from 17.13 % at 250 nm to 15.87 % at 340nm which increases to 18.02 % at 395 nm in UV region. In VIS region, it ranges from 18.09 % at 400nm to 19.90 % at 700nm while in NIR region, the reflectance values are between 19.84 % at 705 nm and 18.24 % at 800nm. The negative values of reflectance obtained for polyaniline and PANI formed with 0.5 g of iron oxide is due to high absorbing nature of the nanoparticles which results to very low values of reflectance within some regions of the electromagnetic spectrum under consideration.

### 3.1.4.Refractive Index

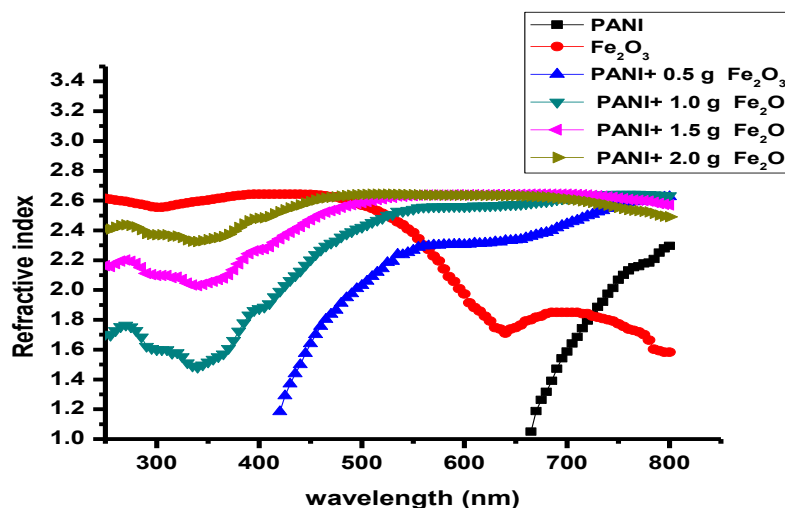


**Figure 5: Plot of Refractive index against wavelength for polyaniline (PANI), iron oxide  $\text{Fe}_2\text{O}_3$  and polyaniline – iron oxide nanocomposites**

Figure 5 shows the refractive index of polyaniline particles, iron oxide nanoparticles and polyaniline – iron oxide nanocomposite respectively. Polyaniline has refractive index ranging

between 1.05 at 665nm and 2.30 at 800nm. The absence of real index of refraction from 250nm to 660 nm for the PANI arises from the negative reflectance observed within these range of wavelength. Iron oxide nanoparticles have refractive index that increases slightly from 2.62 and 2.64 within UV region. In VIS region, the values range from 2.64 to 1.85 while in NIR region, the values are between 1.85 and 1.58. Polyaniline formed with 0.5g of  $\text{Fe}_2\text{O}_3$  has refractive index of 1.18 at 420nm to 2.43 at 700nm. In NIR region, its values range between 2.44 at 705nm and 2.63 at 800nm. Polyaniline formed with 1.0g of  $\text{Fe}_2\text{O}_3$  has refractive index of 1.70 at 250nm to 1.86 at 395nm within UV region. In VIS region, the refractive index values range from 1.88 at 400nm to 2.62 at 700nm. In NIR region, its values range between 2.62 at 705nm and 2.63 at 800nm. Polyaniline formed with 1.5 g of  $\text{Fe}_2\text{O}_3$  has refractive index of 2.16 at 250 nm to 2.26 at 395 nm within UV region. In VIS region, the refractive index values range from 2.27 at 400nm to 2.64 at 700nm. In NIR region, its values range between 2.64 at 705nm and 2.57 at 800nm. Polyaniline formed with 2.0 g of  $\text{Fe}_2\text{O}_3$  has refractive index of 2.41 at 250nm to 2.48 at 395 nm within UV region. In VIS region, the refractive index values range from 2.48 at 400 nm to 2.61 at 700nm. In NIR region, its values range between 2.61 at 705nm and 2.49 at 800nm.

### 3.1.5. Extinction coefficient

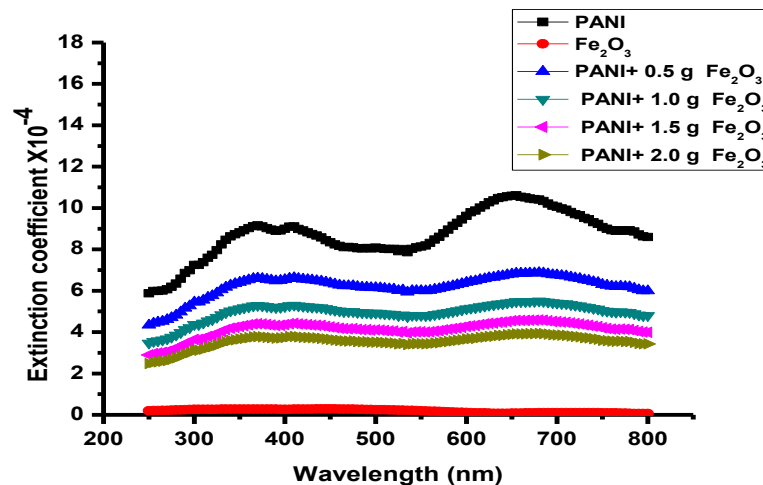


**Figure 6: Plot of Extinction coefficient against wavelength for polyaniline (PANI), iron oxide  $\text{Fe}_2\text{O}_3$  and polyaniline – iron oxide nanocomposites**

Figure 6 shows the graph of extinction coefficient plotted against wavelength for polyaniline, iron oxide and polyaniline iron oxide nanocomposites. Polyaniline nanoparticles has extinction coefficient ranging between  $5.88 \times 10^{-4}$  at 250nm and  $8.91 \times 10^{-4}$  at 395nm within UV region. In VIS region, the values of extinction coefficient range between  $9.00 \times 10^{-4}$  at 400nm and  $10.10 \times 10^{-4}$  at 700nm while in NIR region its values range from  $9.97 \times 10^{-4}$  at 705nm to  $8.59 \times 10^{-4}$  at 800 nm. Iron oxide nanoparticles have extinction coefficient values ranging from  $1.93 \times 10^{-5}$  at 250nm to  $2.71 \times 10^{-5}$  within UV region. In VIS region, the values are between  $2.70 \times 10^{-5}$  and  $1.04 \times 10^{-5}$  at 700nm. In NIR region, the values range from  $1.04 \times 10^{-5}$  at 705nm to  $6.02 \times 10^{-6}$  at 800nm. This result shows that extinction coefficient of iron nanoparticles decreases as wavelength increases. Polyaniline formed with 0.5 g of iron

oxide nanoparticles has extinction coefficient of  $4.34 \times 10^{-4}$  at 250 nm which increase slightly to  $6.49 \times 10^{-4}$  at 395 nm within UV region. In VIS region, the extinction coefficient is between  $6.54 \times 10^{-4}$  at 400nm and slightly increases to  $6.76 \times 10^{-4}$  at 700nm while in NIR region, its values range from  $6.73 \times 10^{-4}$  at 705nm to  $5.99 \times 10^{-4}$  at 800nm. Polyaniline formed with 1.0 g of iron oxide nanoparticles has extinction coefficient of  $3.47 \times 10^{-4}$  at 250 nm which increase slightly to  $5.19 \times 10^{-4}$  at 395 nm within UV region. In VIS region, the extinction coefficient is between  $5.23 \times 10^{-4}$  at 400nm and slightly increases to  $5.41 \times 10^{-4}$  at 700 nm while in NIR region, its values range from  $5.38 \times 10^{-4}$  at 705 nm to  $4.79 \times 10^{-4}$  at 800 nm. Polyaniline formed with 1.5 g of iron oxide nanoparticles has extinction coefficient of  $2.89 \times 10^{-4}$  at 250nm which increase to  $4.33 \times 10^{-4}$  at 395 nm within UV region. In VIS region, the extinction coefficient is between  $4.36 \times 10^{-4}$  at 400nm and slightly increases to  $4.51 \times 10^{-4}$  at 700 nm while in NIR region, its values range from  $4.49 \times 10^{-4}$  at 705nm to  $4.00 \times 10^{-4}$  at 800nm. Polyaniline formed with 2.0 g of iron oxide nanoparticles has extinction coefficient of  $2.48 \times 10^{-4}$  at 250nm which increase slightly to  $3.71 \times 10^{-4}$  at 395 nm within UV region. In VIS region, the extinction coefficient is between  $3.74 \times 10^{-4}$  at 400nm and slightly increases to  $3.86 \times 10^{-4}$  at 700nm while in NIR region, its values range from  $3.85 \times 10^{-4}$  at 705nm to  $3.42 \times 10^{-4}$  at 800nm.

### 3.1.6. Energy Band Gap

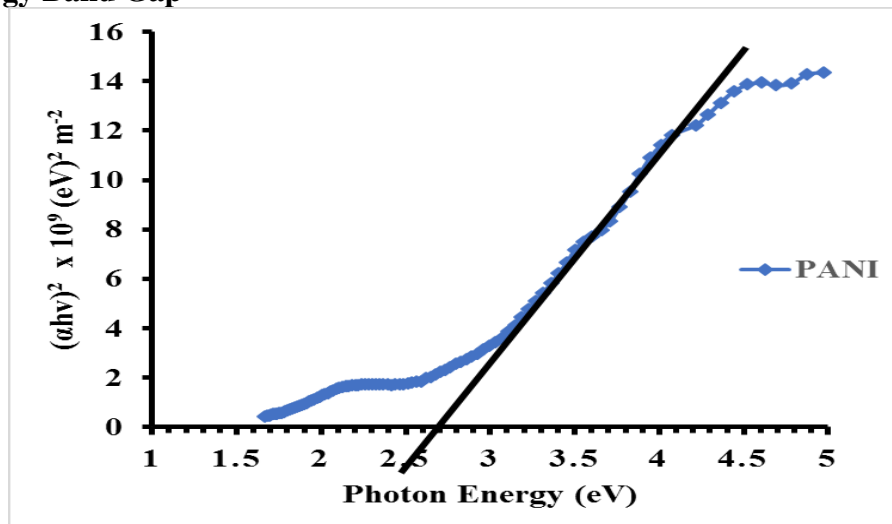
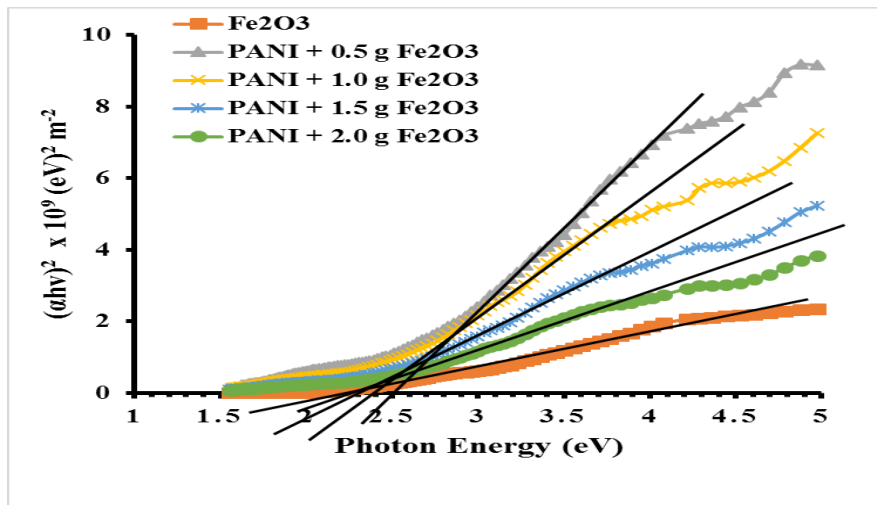


Figure 7: Plot of  $(\alpha h\nu)^2$  against photon energy for polyaniline (PANI), iron oxide  $\text{Fe}_2\text{O}_3$  and polyaniline – iron oxide nanocomposites



**Figure 8: Plot of  $(\alpha h\nu)^2$  against photon energy for iron oxide  $\text{Fe}_2\text{O}_3$  and polyaniline – iron oxide nanocomposites**

Figures 7 and 8 show the plots of  $(\alpha h\nu)$  squared plotted against photon energy  $(h\nu)$ . The direct band gap energy was extrapolated at the axis of the photon energy  $(h\nu)$  where  $(\alpha h\nu)^2 = 0$ . Figure 7 gives the band gaps of 2.69 eV for pure PANI, while Figure 8 gives the band gaps of 2.15 eV for  $\text{Fe}_2\text{O}_3$  nanoparticles, 2.50 eV for PANI / 0.5g  $\text{Fe}_2\text{O}_3$ , 2.40 eV for PANI / 1.0g  $\text{Fe}_2\text{O}_3$ , 2.27 eV for PANI / 1.5g  $\text{Fe}_2\text{O}_3$  and 2.20 eV for PANI / 2.0g  $\text{Fe}_2\text{O}_3$  nanocomposites respectively. Band gap energy value obtained for pure polyaniline is in agreement with 2.70 eV obtained by (Salma, 2013). Paul – Nwokocho and Ozumba (2018) obtained energy band gap of 2.75 eV for pure polyaniline. Gilbert *et al.*, (2009) obtained an energy band gap of 2.20 eV for  $\text{Fe}_2\text{O}_3$  and Balaraju *et al.*, (2017) obtained an energy band gap of 2.08 eV. These results are in line with our result of 2.15 eV.

From Figure 8, it can be seen that the optical band gap of polyaniline iron oxide nanocomposites decreased from 2.50 eV to 2.20 eV as amount of  $\text{Fe}_2\text{O}_3$  increased. The decrease in the optical band gap may be due to reduction in the disorder of the system and increase in the density of defect states (Reda and Al – Ghannam, 2011) and modifications of the polymer matrix due to the addition of dopant (Mansour *et al.*, 2015). Shumaila *et al.*, (2013) observed a similar decrease in the energy band gap of polyaniline when intercalated with selenium nanowires. They suggested that the decrease in band gap may be due to the broadening of polaron bands, which is attributed to the increase in carrier concentration in the polymer after doping. A similar behavior of decrease in band gap was obtained for polyaniline doped with increasing Zirconium nanoparticles concentrations (Gupta *et al.*, 2011). According to Gupta *et al.*, (2011), this decrease in band gap as zirconium concentration increases caused an increase in electrical conductivity of the polyaniline. Corresponding results were observed by other researchers such as (Saleh *et al.*, 2018; Cabuk and Gunduz, 2017; Dhachanamoorthi *et al.*, 2017; Sharma *et al.*, 2014 and Saleh *et al.*, 2009) for various doping agents. The values of the optical band gap for polyaniline nanoparticle, iron oxide nanoparticles and polyaniline – iron oxide nanocomposites are suitable for application in semiconducting materials.

## 5. CONCLUSION

Polyaniline nanoparticles, iron oxide nanoparticles and polyaniline-iron oxide nanocomposites were successfully synthesized using chemical processes. Polyaniline nanoparticle were synthesized by chemical polymerization of aniline monomer and iron oxide nanoparticles were synthesized by co – precipitation of two iron precursors of  $\text{Fe}^{3+}$  and  $\text{Fe}^{2+}$  compounds. The polyaniline metal oxide nanocomposites formed were achieved by dispersion of the synthesized metal oxide on the reaction bath before the on – set of polymerization. All the synthesized particles formed were heat treated to remove water and other solvents such as ethanol. The samples formed were subjected to optical characterization. The optical properties of polyaniline nanoparticles, iron oxide nanoparticles and polyaniline – iron oxide nanocomposites reveal good results which are comparable with results obtained by other researcher. The change in the optical properties of polyaniline on addition of metal oxide may be as a result of good interaction between the particles of the polyaniline and that of metal oxide. These results obtained suggest the possibility of using the material in optoelectronics devices like LEDs, solar cells, transducers, and photodetectors.

## REFERENCES

- Abdulla, H. S. and Abbo, A. I. (2012). Optical and electrical properties of thin films of polyaniline and polypyrrole. *International Journal of Electrochemical Science*, 7, 10666 – 10678.
- Al – Daghman, A. N. J. (2019). Optical properties of conducting polyaniline doped by  $\text{H}_2\text{SO}_4$ . *Journal of Scientific and Engineering Research*, 6(1), 50 – 54.
- Technology, 2(12), 7068 – 7072.
- Balamurugan M G, Mohanraj S, Kodhaiyolii S, Pugalenthi V (2014). *Ocimum sanctum* leaf extract mediated green synthesis of iron oxide nanoparticles: spectroscopic and microscopic studies, *Journal of Chemical and Pharmaceutical Sciences*, 2014(69), 201 – 204.
- Balaraju, B., Kuppan, M., Babu, S. H., Kaleemulla, S., Rao, N. M., Krishnamoorthi, C., Joshi, G. M., Rao, G. V., Subbaravamma, K., Omkaram, I. and Reddy, D. S. (2017). Structural, Magnetic Properties of Wide Band Gap Oxide Semiconductors. *Mechanics, Materials Science and Engineering*, 9(1), 132 – 136.
- Businova, P., Chomoucka, J., Prasek, J., Hrdy, R., Drbohlavova, J., Sedlacek, P. and Hubalek, J. (2011). Polymer-Coated Iron Oxide Magnetic Nanoparticles – Preparation and Characterization. *Nanoconference*, 21. – 23. 9, Brno, Czech Republic, EU
- Cabuka M. and GündüzB., (2017). Controlling the optical properties of polyaniline doped by boric acid particles by changing their doping agent and initiator concentration. *Journal of Applied Surface Sciences*, 424(3), 345 – 351.
- Canales, M., Torras, J., Fabregat, G., Meneguzzi, A. and Aleman, C. (2014). Polyaniline Emeraldine salt in the amorphous solid state; Polaron versus Bipolaron. *The journal of Physical Chemistry B*. 118(39), 11552 – 11562.
- De – Freitas, J. C., Branco, R. M., Lisboa, I. G. O., Da – Costa, T. P., Campos, M. G. N., Júnior, M. J. and Marques R. F. C. (2015). Magnetic Nanoparticles Obtained by Homogeneous Coprecipitation Sonochemically Assisted. *Materials Research*. 18(2), 220 – 224.
- Dhachanamoorthi, N., Chandra, L., Suresh, P. and Perumal, K., (2017). Facile Preparation and Characterization of Polyaniline-iron Oxide Ternary Polymer Nanocomposites by Using

- “Mechanical Mixing” Approach. *Mechanics, Materials Science and Engineering*, 9(2), 273 – 280.
- Farahmandjou M. and Soflaee F. (2015). Synthesis and Characterization of  $\alpha$ -Fe<sub>2</sub>O<sub>3</sub> Nanoparticles by Simple Co - precipitation Method, *Physical Chemistry Research*, 3(3), 191 – 196.
- Gilbert, B., Frandsen, C., Maxey, E. R. and Sherman, D. M. (2009). Band-gap measurements of bulk and nanoscale hematite by soft x-ray spectroscopy. *Physical Review B*, 79(035108), 1 – 7.
- Gul, S., Ali – Shah, A. and Bilal, S. (2013). Synthesis and characterization of processable polyaniline salts. *Journal of Physics: Conference Series*, 439(012002), 1 – 11.
- Gupta, K., Jana, P. C. and Meikap, A. K. (2011). Synthesis, electrical transport and optical properties of polyaniline – zirconium nanocomposite. *Journal of Applied Physics*, 109(123713), 1 – 9.
- Hassan, D., Khalil, A. T., Saleem, J., Diallo, A., Khamlich, S., Shinwari, Z. K. and Maaza, M. (2018). Biosynthesis of pure hematite phase magnetic iron oxide nanoparticles using floral extracts of *Callistemon viminalis* (bottlebrush): their physical properties and novel biological applications. *Artificial cells, nanomedicine, and biotechnology*, DOI: 10.1080/21691401.2018.1434534.
- Kostyukova, D. and Chung, Y. H. (2016). Synthesis of Iron Oxide Nanoparticles Using Isobutanol. *Journal of Nanomaterials*, 2016(4982675), 1 – 9.
- Majid K., Awasthi S., Singla M.L., (2007) *Sensor Actuators A* 135, 113–118;
- Mota, M. L., Carrillo, A., Verdugo, A. J., Olivas, A., Guerrero, M. J., Cruz, E. C. and Ramirez, N. N. (2019). Synthesis and novel purification process of PANI and PANI/Ag NPs composites. *Molecules*, 24(1621), 1 – 13.
- Paul-Nwokocha, O. N. and Ozuomba, J. O. (2018). Synthesis and Optical Characterization of Acid-Doped Polyaniline Thin Films. *Nigerian Journal of Technology*, 37 (1), 135 – 138
- Reddy K. R, Lee K.P., Iyengar A.G., (2007). *J. Polym. Appl. Sci.* 104, 4127–4134.
- Thanpitcha, T., Sirivat, A., Jamieson, A. M. and Rujiravanit, R. (2008). Synthesis of polyaniline nanofluids using an in – situ seeding techniques. *Synthetic metals*, 158, 695 – 703.
- Tang B.Z., Geng Y., Lam J.W., Li B., Jing X., Wang X., Wang F., Pakhomov A.B., Zhang X.X., (1999), *Chem. Mater.* 11, 1581
- Vadiraj, K, and Belagal, S. (2015). Characterization of Polyaniline for Optical and Electrical properties. *Journal of Applied Chemistry*, 8(1), 53 – 56.
- Wasfi, A. S., Humud, H. R., Abed, M. A. and Ismael, M. E. (2017). Preparation of Polyaniline/Zinc Oxide Nanocomposite Thin Films by Microwave Plasma. *International Journal of ChemTech Research*, 10(5), 886 – 892.
- Yang, X., Zhao, T., Yu, Y. and Wei, Y. (2004). Synthesis of conductive polyaniline/epoxy resin composite; doping of the interpenetrating network. *Synthetic metals*, 142, 57 – 61.
- Yang, Y., Ding, Y., Chen, G. and Li, C. (2007). Synthesis of conducting polyaniline using novel anionic Gemini surfactant as micellar stabilizer. *Euro. Polymer Journal*, 43, 3337 – 3343.
- Yin, W. and Ruckenstein, E. (2000). Soluble polyaniline co – doped with Dodecylbenzene sulfonic acid and hydrochloric acid. *Synthetic metals*, 108, 39 – 46.